Soil water retention and hydraulic conductivity measured in a wide saturation range

Tobias L. Hohenbrink[1,2], Conrad Jackisch[3,4], Wolfgang Durner[1], Kai Germer[1,5], Sascha C. Iden[1], Janis Kreiselmeier[6,7], Frederic Leuther[8,9], Johanna C. Metzger[10,11], Mahyar Naseri[1,5], Andre Peters[1]

[1] Institute of Geoecology, Soil Science & Soil Physics, TU Braunschweig, Braunschweig, 38106, Germany
[2] Deutscher Wetterdienst (DWD), Agrometeorological Research Center, Braunschweig, 38116, Germany
[3] Interdisciplinary Environmental Research Centre, TU Bergakademie Freiberg, Freiberg, 09599, Germany
[4] Institute for Water and River Basin Management, Chair of Hydrology, Karlsruhe Institute of Technology (KIT), Karlsruhe, 76131, Germany
[5] Thünen Institute of Agricultural Technology, Braunschweig, 38116, Germany
[6] Thünen Institute of Forest Ecosystems, Eberswalde, 16225, Germany
[7] Institute of Soil Science and Site Ecology, TU Dresden, Tharandt, 01737, Germany
[8] Helmholtz Centre for Environmental Research - UFZ, Department of Soil System Sciences, Halle (Saale), 06120, Germany
[9] Chair of Soil Physics, University of Bayreuth, 95447 Bayreuth, Germany
[10] Institute of Soil Science, Center for Earth System Research and Sustainability (CEN), Universität Hamburg, Hamburg, 20146, Germany
[11] Institute of Geoscience, Group of Ecohydrology, Friedrich Schiller University Jena, Jena, 07749, Germany

Correspondence to: Tobias L. Hohenbrink (t.hohenbrink@tu-braunschweig.de)

Abstract. Soil hydraulic properties (SHP), particularly soil water retention capacity and hydraulic conductivity of unsaturated soils, are among the key properties that determine the hydrological functioning of terrestrial systems. Some large collections of SHP, such as the UNSODA and HYPRES databases, already exist for more than two decades. They have provided an essential basis for many studies related to the critical zone. Today, sample-based SHP can be determined in a wider saturation range and with higher resolution by combining some recently developed laboratory methods. We provide 572 high-quality SHP data sets from undisturbed, mostly central European samples covering a wide range of soil texture, bulk density and organic carbon content. A consistent and rigorous quality filtering ensures that only trustworthy data sets are included. The data collection contains: (i) SHP data: soil water retention and hydraulic conductivity data, determined by the evaporation method and supplemented by retention data obtained by the dew point method and saturated conductivity measurements, (ii) basic soil data: particle size distribution determined by sedimentation analysis and wet sieving, bulk density and organic carbon content, as well as (iii) metadata including the coordinates of the sampling locations. In addition, for each data set, we provide soil hydraulic parameters for the widely used van Genuchten-Mualem model and for the more advanced Peters-Durner-Iden model. The data were originally collected to develop and test SHP models and associated pedotransfer functions. However, we expect that they will be very valuable for various other purposes such as simulation studies or correlation analyses of

different soil properties to study their causal relationships. The data is available under the DOI link https://doi.org/10.5880/fidgeo.2023.012 (Hohenbrink et al., 2023; the final DOI will be registered before publication, please use the review link meanwhile: https://dataservices.gfz-potsdam.de/panmetaworks/review/5c617cd2664ea4d03e81301b5bc2236f1948a3cf7eb9bad48da940524f0cbac0).

1 Introduction

A sound understanding of the hydrological functioning of variably saturated soils in the environmental cycles is important for numerous applications in agronomy, forestry, water management and other disciplines. The hydrological functioning of soils is controlled by the soil hydraulic properties (SHP), specifically the water retention and hydraulic conductivity characteristics. SHP models are essential to simulate water dynamics, solute transport and energy transfers in the vadose zone using water flow and transport equations. Such SHP models are empirical mathematical representations of the highly non-linear soil hydraulic curves, which are parameterised based on measured SHP data. In order to estimate SHP from more accessible information, pedotransfer functions relate SHP parameters to basic soil properties like soil texture, bulk density, and organic carbon content (C_{org}) (Vereecken et al., 2010; Van Looy et al., 2017).

Since the early applications of SHP models in hydrological simulations in the 1980s, there is a demand for such parameters (Carsel and Parrish, 1988). Commonly, they are derived for specific SHP models (Vereecken et al., 2010), which is most often the van Genuchten-Mualem model (Van Genuchten, 1980; Mualem, 1976). Fitting non-linear SHP models to observed data and developing pedotransfer functions both require large data collections containing information about SHP measured over a large range of saturation in samples with various combinations of basic soil properties. Such data collections are commonly based on individual soil samples from various profiles.

Due to methodological restrictions, data for such applications were first limited to few points on the soil water retention curve using ceramic pressure plate extractors and pressure-controlled hydraulic conductivity (Brooks and Corey, 1964). Since the late 1990s, different data collections of SHP and associated basic soil properties have been compiled. They formed the basis to develop various pedotransfer functions. The freely available Unsaturated Soil Hydraulic Database (UNSODA) provided by the U.S. Department of Agriculture comprises nearly 800 SHP data sets from disturbed and undisturbed samples (Nemes et al., 2001). It includes measurements of retention and hydraulic conductivity with different coverage of the saturation range as well as basic soil properties, e.g. information on soil texture or bulk density. UNSODA was an important basis to develop ROSETTA (Schaap et al., 2001; Zhang and Schaap, 2017), which is the most established pedotransfer function to predict the parameters of the van Genuchten-Mualem SHP model.

Another prominent large collection of retention and hydraulic conductivity data is the database of the Hydraulic Properties of European Soils (HYPRES) (Wösten et al., 1999) and its further development as the European Hydropedological Data Inventory (EU- HYDI) (Weynants et al., 2013) which is unfortunately not freely available. There are a few more specific SHP data collections, e.g. the HYBRAS data describing Brazilian soils (Ottoni et al., 2018), and the collection by Schindler and Müller

67 (2017) which contains only data measured with the evaporation method (Peters and Durner, 2008; Schindler, 1980). Recently,

68 Gupta et al. (2022) gathered published soil water retention data from 2,702 sites, prepared them for use in land surface modeling

69 and made them openly accessible.

70 The existing databases have undoubtedly supported a large number of hydrological studies leading to important conclusions,

71 but they still have some limitations and shortcomings. Often, SHP data only cover a small part of the naturally occurring range

72 of soil saturation. Gupta et al. (2022) emphasised that in many cases the retention data series contain only a few pairs of data

73 and lack information in the wet region close to full saturation. Measured saturated hydraulic conductivity (K_{sat}) is included in

74 several data collections, but detailed information about the unsaturated hydraulic conductivity is still rare.

75 It is technically possible to create pedotransfer functions using only retention and K_{sat} data (Assouline and Or, 2013) as has

76 often been done in the past. However, in such cases the shape of the hydraulic conductivity curves is predicted only from the

77 water retention curve and scaled to match K_{sat}. Hence, the absolute position of the conductivity curve is solely determined by

78 a single K_{sat} value, which is strongly influenced by soil structure and macropore connectivity, which are often not recorded nor

79 assessed at the time of sampling.

80 A serious development and rigorous testing of full-range SHP models always requires measured unsaturated hydraulic

81 conductivity data. Zhang et al. (2022) showed impressively how fast a supposedly large number of available SHP data sets can

82 collapse, when they are filtered by predefined data requirements. They initially gathered 19,510 data sets from established data

83 collections and first narrowed it down to 14,997 data sets describing undisturbed samples. They then extracted 1,801 lab

84 measured data sets with information about both soil water retention and hydraulic conductivity. Finally, they extracted data

85 sets with at least six retention and seven conductivity data pairs, each of which contained at least three data pairs close to

86 saturation at matric heads larger than -20 cm. They ended up with 194 data sets accounting for only 1 % of the initial number.

87 Given the wide variability of naturally occurring soils, many pedotransfer functions are based on data collections that contain

88 rather limited soil information. Weihermüller et al. (2021) showed that the choice of the pedotransfer function used in a soil

89 hydrological model can have considerable effects on simulated water fluxes. The artificial neural network behind ROSETTA

90 has been trained with 2,134 retention curves, 1,306 K_{sat} values and 235 unsaturated conductivity curves (Schaap et al., 2001;

91 Zhang and Schaap, 2017). Considering the wide use of ROSETTA with more than 1,840 citations (retrieved from Scopus on

92 02/07/2023) it becomes apparent that the specific characteristics of only 235 unsaturated hydraulic conductivity data sets have

93 been propagated into a large number of applications and conclusions.

94 However, pedotransfer functions can only predict the SHP within the range covered by the training dataset. Furthermore, they

95 tend to reflect the individual characteristics of the training data, which are most pronounced in case of small databases. To

96 prevent such bottleneck effects, the basis for pedotransfer applications needs to be further diversified. This requires new and

97 independent, quality-assured SHP data collections. With advanced measuring techniques becoming standard in many soil

98 physical laboratories, it is now much easier to obtain experimental SHP data over a wider range of soil moisture and in the

99 desired high quality.

In this paper, we present a collection of 572 new data sets of soil properties measured in soil samples (Hohenbrink et al., 2023) that are independent of existing databases. Each data set contains (i) SHP, and (ii) basic soil properties such as soil texture, bulk density and C_{org}. The SHP data meet high quality requirements since they have been determined by combining state-of-the-art laboratory techniques, i.e. the evaporation method (Peters and Durner, 2008; Schindler, 1980), the dewpoint potentiometry (Campbell et al., 2007), and separate K_{sat} measurements. In addition, each dataset has undergone thorough quality control. The data collection covers a wide range of soil textures. Soil texture information is provided according to both the German (Ad-hoc-Arbeitsgruppe Boden, 2005) and the USDA classification systems (USDA, 1999). Within the silt and sand classes, we also provide the sub-classes coarse, medium and fine according to the German system.

In support of the FAIR principles (Wilkinson et al., 2016), we provide free access to the data for the development of SHP models and pedotransfer functions. We expect them to be valuable for a variety of purposes such as simulation studies and statistical analyses of various soil properties.

2 Materials and Methods

2.1 Data sources

A community initiative for collecting and sharing consistent SHP data was launched by researchers from the Division of Soil Science and Soil Physics at TU Braunschweig. Scientists from four other institutions participated by providing data measured in their laboratories. Most of the data had already been used to answer individual research questions at various research sites (Jackisch et al., 2017; Kreiselmeier et al., 2019, 2020; Leuther et al., 2019; Jackisch et al., 2020; Germer and Braun, 2019; Metzger et al., 2021). Some existing but yet unpublished data sets have been reviewed and integrated into the data collection, too. In addition, we systematically added data from sites with soil characteristics that were missing from the data collection. Such data were explicitly measured for this data collection.

To be included in the data collection, the data sets had to contain soil water retention and hydraulic conductivity data, measured in the laboratory by the evaporation method, preferably supplemented by dewpoint method data and also measurements of saturated hydraulic conductivity. The data sets also had to include information about soil texture, and bulk density, and preferably C_{org}. We have aimed to cover the data space of these basic soil properties as completely as possible. Therefore, we also included data sets that lacked some of the preferred information, when they added new combinations of basic soil properties to the data collection.

2.2 Soil samples

Each data set is based on one undisturbed soil sample taken in situ with metal cylinders. In 542 cases the sample volume was 250 cm^3, while 30 samples had a volume of 692 cm^3 as indicated in the metadata table of Hohenbrink et al. (2023). For the measurement of C_{org}, soil texture and retention data in the dry range (dewpoint method), disturbed soil (sub)samples were taken. In 363 cases, exactly one disturbed sample was assigned to each undisturbed sample, either by taking both samples in

close proximity to each other or by taking the disturbed sample directly from the undisturbed sample material after measuring the SHP. In the other 209 cases, the disturbed sample was taken as mixed material, representative for an entire site with several undisturbed sampling points. Consequently, in the latter cases the soil variables derived from the aggregated disturbed samples have been assigned to more than one data set (indicated in the metadata table). Information about the positions of the sampling sites is available for 555 data sets. It has either been measured by GPS or was taken from aerial images after sampling. The geo-positions are reported with a lateral accuracy of 100 m, which represents the best accuracy class in Gupta et al. (2022). The sampling depth is reported for 474 samples in the metadata table.

2.3 Laboratory measurements

Soil water retention in the wet (defined here as pF < 1.8; $pF = log_{10}(-h\ [cm])$) and medium (defined here as 1.8 < pF < 4.2) moisture range and hydraulic conductivity in the medium moisture range were simultaneously determined with the simplified evaporation method (Peters and Durner, 2008; Schindler, 1980) using the HYPROP device (METER Group, AG, Germany). The evaporation method provides information related to the drying branches of the SHP curves. The air entry points of the tensiometer cups were used as an additional measuring point (Schindler et al., 2010) in cases where the duration of the evaporation experiments was long enough. Soil water retention information was supplemented mainly in the dry moisture range (defined here as pF > 4.2) by measurements with the dewpoint method (Campbell et al., 2007; Kirste et al., 2019) using the WP4C device (METER Group, Inc., USA). Hydraulic conductivity of the saturated soil was measured in the undisturbed samples either with the falling head or the constant head method using the KSAT device (METER Group, AG, Germany). Particle size distributions of the disturbed soil samples were determined by wet sieving for the sand fractions and sedimentation methods for the silt fractions and clay content (DIN ISO 11277, 2002). The sedimentation analyses were carried out with slightly different approaches in each lab as specified for each dataset in the metadata table. The respective particle size classes were defined by the German soil classification system (Ad-hoc-Arbeitsgruppe Boden, 2005). Because the German system differs from international standards in the boundary between silt and sand (German: 63 µm, USDA: 50 µm) we additionally converted the texture data by interpolation with monotone cubic splines fitted to the cumulative particle size distributions as recommended by Nemes et al. (1999). Illustrations showing data in the texture triangle were created using the "soiltexture" R-package (Moeys, 2018). Bulk density of each sample was determined by oven-drying for at least 24 h after the evaporation experiments. C_{org} was determined with high-temperature combustion using different elemental analysers, which are listed in the metadata table.

2.4 Data preparation and quality check

The results of all SHP measurements have been compiled with the HYPROP-FIT software (Pertassek et al., 2015). It was developed to organise and evaluate raw data from the simplified evaporation method, the dewpoint potentiometry and individual K_{sat} measurements.

162 Despite a high level of automation and standardisation, manual adjustments to selecting the raw data for evaluation is required.

163 To avoid misalignment due to differences in the manual treatment, all resulting retention and hydraulic conductivity points

164 have been re-checked for plausibility by the same expert based on the following procedure:

165   1.   Tensiometer check and offset correction: HYPROP uses two tensiometers at different levels. If in the first hours of

166   the experiments (close to saturation) the measured difference between the upper and lower tensiometers deviate from

167   the actual difference of 2.5 cm by more than 1 cm, an offset correction was performed to prevent unrealistic hydraulic

168   gradients during data evaluation.

169   2.   Consistency check if the initial water content was smaller than the porosity: If not, a slightly larger column height (1

170   - 4 mm) has been assumed to account for surplus water in the data evaluation.

171   3.   Setting the evaluation limits of the evaporation method: Because not all measurements follow idealistic conditions,

172   the data for evaluation have been limited to plausible records (capillary connection of the tensiometers, plausible

173   upward gradient, omission of scattered values for unsaturated conductivity near saturation).

174   4.   Omit retention data of the dewpoint potentiometry outside its validity limits: dewpoint potentiometry measurements

175   tend to be less precise for lower tensions. To avoid unnecessary variance between the different methods (dewpoint

176   and evaporation), values below pF 4 were omitted.

177   5.   Plausibility of hydraulic conductivity values: In cases of values for unsaturated conductivity exceeding the separately

178   measured saturated conductivity, such values were omitted.

179   6.   Visual alignment check for data from the three methods (K_{sat}, evaporation, dewpoint) and omission of obviously

180   misaligned datasets from the collection.

181 The original binary HYPROP-FIT files are provided by Hohenbrink et al. (2023) to ensure transparency on all manual

182 adjustments. The final series of measured retention and hydraulic conductivity data were exported from HYPROP-FIT to csv-

183 files for further data processing, which was mainly performed in R (R Core Team, 2020).

2.5 Fitting models to measured SHP data

185 For direct access to resulting SHP model parameters, we fitted two models to the measured soil water retention and hydraulic

186 conductivity data using a shuffled complex evolution (Duan et al., 1992) in SHYPFIT 2.0 (Peters and Durner, 2015). The first

187 model is the well-established van Genuchten-Mualem (VGM) model (Van Genuchten, 1980; Mualem, 1976). The second

188 model is the recent version of the Peters-Durner-Iden (PDI) model with the VGM model as the basic function (Peters et al.,

189 2021, 2023).

190 The PDI model specifically considers (i) capillary water in completely filled pores and (ii) non-capillary water in thin films on

191 particle surfaces and in corners and ducts of the pore system. The explicit consideration of non-capillary water yields more

192 realistic retention and hydraulic conductivity curves in the medium and dry moisture range. Furthermore, the description of

193 hydraulic conductivity in the dry range includes an effective component that reflects isothermal vapour flux (Peters, 2013).

194 Retention and conductivity parameters were estimated simultaneously. During model fitting the few retention points measured
195 with the dewpoint method were weighted ten times higher than those obtained with the evaporation method because the latter
196 have a much higher abundance. Weights of hydraulic conductivity data were defined in a way that their ratio to the mean
197 retention data weights was 16 to 10,000 following Peters (2013). We neglected measured K_{sat} values in the parameter
198 optimization process, since they mainly reflect effects of soil structure (Weynants et al., 2009), which is not considered in the
199 unimodal SHP models. The saturated hydraulic conductivity model parameter K_s equals the hydraulic conductivity of the
200 saturated bulk soil excluding the soil macropore network.

201 For the VGM model six parameters were estimated (residual and saturation water content θ_r (-) and θ_s (-), the shape parameters
202 α (cm^{-1}) and n (-), the tortuosity parameter λ (-), and the saturated hydraulic conductivity parameter K_s (cm d^{-1})). The predefined
203 parameter limits are listed in Table 1. The upper limits for θ_r and θ_s were defined as a fraction of porosity Φ to ensure physical
204 consistency. For the PDI model, five parameters (θ_r, θ_s, α, n and λ) were estimated with the same settings and fitting algorithms
205 as in Peters et al. (2023).

206 Unlike VGM and common models of SHP, where the relative hydraulic conductivity curve is scaled by the saturated
207 conductivity K_s, the new PDI model structure allows to realistically predict conductivity data close to saturation, which are
208 usually not available (Peters et al., 2023). To avoid an unrealistically sharp drop of the conductivity curve close to saturation
209 for soils with wide pore size distribution, we constrained the conductivity model by a maximum pore radius (maximum tension)
210 close to saturation with the "h-clip approach" (Iden et al., 2015). According to Jarvis (2007), the maximum tension was set to
211 -6 cm (5 mm equivalent pore diameter). The saturated conductivity is defined as the predicted absolute conductivity at this
212 tension. We refer to Peters et al. (2021, 2023) for a more detailed description of the applied version of the PDI model.

213 **Table 1: Upper and lower parameter boundaries for fitting the van Genuchten-Mualem model (VGM) and the Peters-Durner-Iden**
214 **model (PDI). α and n: shape parameters, θ_r and θ_s: residual and saturation water content, Ks: saturated hydraulic conductivity**
215 **parameter, λ: tortuosity parameter. Note that the parameter boundaries for θ_r and θ_s are defined individually as a fraction of the**
216 **porosity Φ. The boundaries for θ_r and λ differ between both models to ensure physical consistency. The lower λ constraint for VGM**
217 **is set to guarantee physical consistency while allowing for maximum flexibility.**

	VGM		PDI	
	lower	upper	lower	upper
α (cm^{-1})	10^{-5}	0.5	10^{-5}	0.5
n (-)	1.01	8.00	1.01	8.00
θ_r (-)	0.0	$0.25 \cdot \Phi$	0.0	$0.75 \cdot \Phi$
θ_s (-)	0.2	Φ	0.2	Φ

K_s (cm d^{-1})	10^{-2}	10^5	-	-
λ (-)	$1 - \dfrac{2}{1 - \dfrac{1}{n}}$	10	-1	10

3 Data description

The data collection is structured in the following sections: (i) metadata (file: MetaData.csv), (ii) basic soil properties (BasicProp.csv), and (iii) SHP including measured points of the retention curve and hydraulic conductivity curve (RetMeas.csv, CondMeas.csv), (iv) optimized parameter sets for two SHP models (Param.csv) and (v) data series resulting from both SHP models (HydCurves.csv). Each dataset is labelled by a unique Sample-ID for easy joining of the different tables.

3.1 Metadata

The metadata table summarizes relevant information about the availability of the single variables in each data set. All 572 datasets contain SHP measurements by the evaporation method, 499 contain at least one dew point measurement and 409 data sets include K_{sat} measurements (Table 2). In 370 data sets all three kinds of SHP information are available. In case of the basic soil properties, soil texture and bulk density are available for all datasets and C_{org} is available in 488 cases. Complete information about all variables (SHP and basic soil properties) is contained in 315 data sets (57 %).

The data collection contains location information for 555 data sets (see Appendix Figure A1). The sampling sites are not arranged systematically, as the region of sampling has not been a criterion for data collection. They are rather clustered in the regions where the contributing groups have performed field work. Most of the samples have been taken in Central Europe ($n = 508$). Few data sets come from Canada ($n = 29$), Japan ($n = 5$) and Israel ($n = 30$).

Table 2: Key variables contained in the data collection, laboratory method used for analyses and number of available samples.

Measured variable	Laboratory method	Number of available samples
Hydraulic Properties of	Evaporation method (HYPROP)	572

unsaturated soil	Added measurements by air entry point of tensiometer (Schindler et al., 2010)	286
	Added retention measurements by dew point method (Campbell et al., 2007)	499
Hydraulic conductivity of saturated soil	Falling head or constant head method	409
Bulk density	Weight of oven dried (105°C) undisturbed samples	572
Soil texture (63…2000 µm)	Wet sieving with 2000, 630, 200, 63 µm sieves	572
Soil texture (≤ 63 µm)	Pipette method (Köhn, 1931)	300
	Pipette method (Moshrefi, 1993)	78
	Hydrometer method	52
	Integral suspension pressure method (Durner et al., 2017, Durner and Iden, 2021)	94
	Method unknown	48
Soil organic carbon content	High-temperature combustion	488

3.2 Basic soil properties

The data collection covers a wide range of soil textures, including soils with up to 65 % clay and 93 % silt and 100 % sand (positions of symbols in the soil texture triangle, Figure 1). It covers the textures most frequently found in temperate climates. The main textural classes according to the German classification (Ad-hoc-Arbeitsgruppe Boden, 2005) account for 217 (sand), 146 (silt), 121 (loam) and 88 (clay) data sets (Figure 1a). The sandy soils are further subdivided into 39 samples for pure sand and 178 samples for loamy sand, as the SHP usually have the highest variation within the sand texture class. The two areas in the soil texture triangle with the lowest data coverage are sandy clay and sandy silt. Figure 1d shows the colour coded samples in the USDA texture triangle to provide orientation for international readers.

The bulk density of the samples varies between 0.37 g cm^{-3} and 1.89 g cm^{-3} with a median of 1.40 g cm^{-3}. High bulk density mainly occurs in sandy soils while silty clay soils are less dense (Figure 1b and 1e). In general, soil bulk density scatters across

248 the texture triangle, which is reflected by rather weak but significant Pearson correlations (p-value <0.05) between bulk density

249 and the sand ($r = 0.41$), silt ($r = -0.24$) and clay ($r = -0.50$) contents, respectively.

250 C_{org} in the samples ranges from 0.04 % to 19.26 % with a median of 1.44 %. The maximum values occur mainly in silty clay,

251 loam and silty sand soils. Smaller C_{org} values are associated with sand and silt soils (Figure 1c and 1f).

252 In addition to the standard soil texture classification by sand, silt and clay fractions, the subgroups for silt and sand (i.e. coarse

253 sand, medium sand, fine sand, coarse silt, medium silt, and fine silt) are provided for the German classification system (Figure

254 2a). Most silt soils contain a maximum fraction of coarse silt (20 µm - 63 µm), while the loamy sands are mainly dominated

255 by the fine sand fraction (63 µm - 200 µm). In contrast to the weak correlation between soil texture with C_{org} and bulk density,

256 the latter are negatively correlated to each other (r=-0.76; Figure 2b).
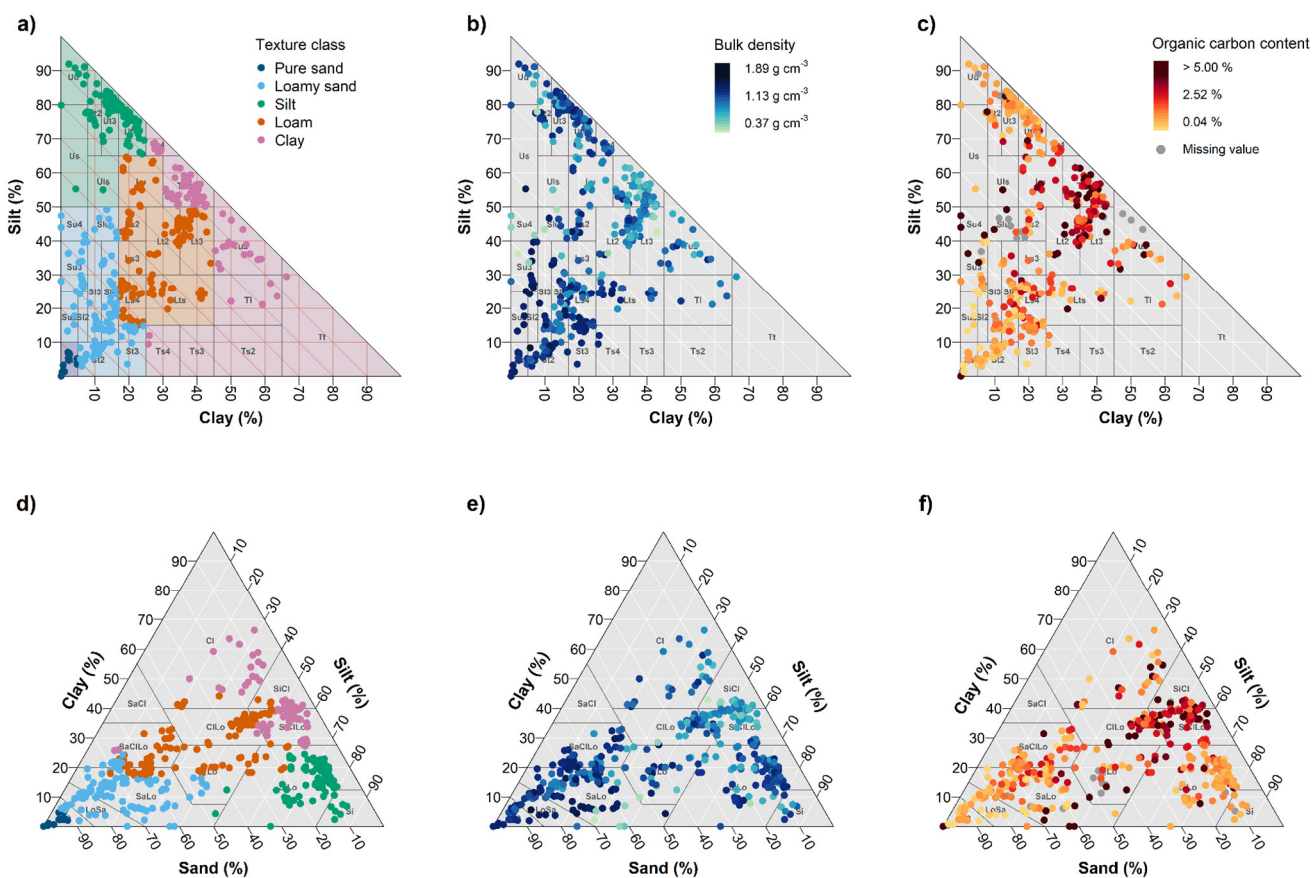
257

258 **Figure 1: Distributions of (a, d) texture classes, (b, e) bulk density and (c, f) organic carbon content in the texture triangle of the**
259 **German (a-c) and USDA (d-f) systematic.**

260

261

262
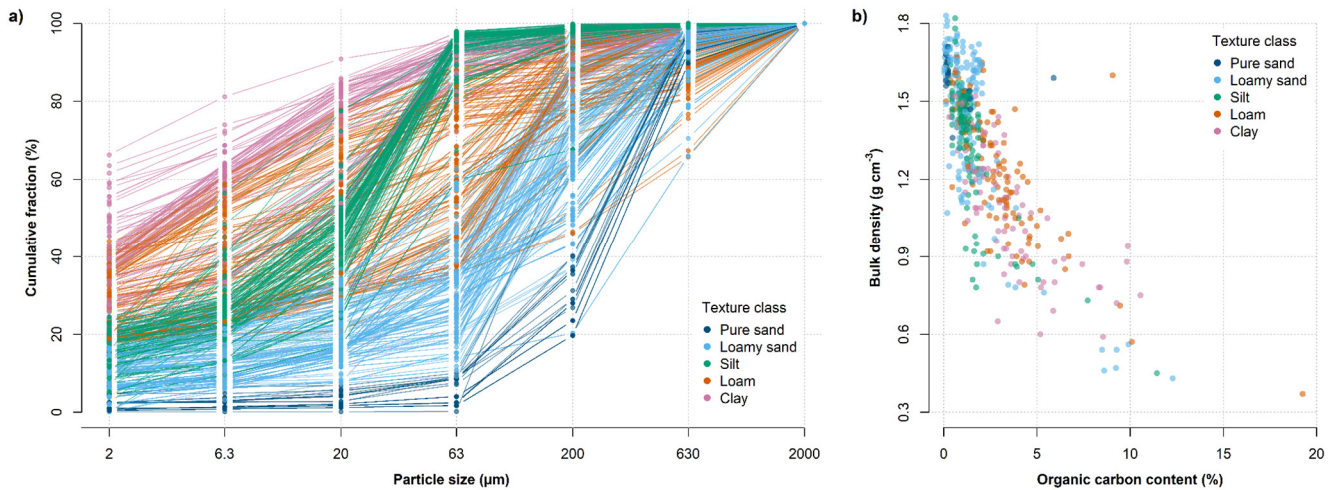
263

264 **Figure 2: a) Cumulative particle size distributions of the 572 samples (German classification system). b) Scatterplot of C_{org} and bulk**
265 **density (r=-0.76). The reference texture classes are colour coded.**

266 **3.3 Measured soil hydraulic data**

267 The measured SHP are shown in Figure 3. The retention data cover almost the entire range between full water saturation and
268 oven dryness. The highest data coverage is available in the wet and medium saturation range with pF < 3.2, where the data
269 stem from the simplified evaporation method. Half of the datasets contain one additional data point between pF 3.0 and pF 4.0
270 which originates from the air entry pressure of the porous tensiometers cup. In 499 data sets at least one data pair between pF
271 4.0 and pF 6.3 determined by the dewpoint method exists. To cover the drying branch towards pF 6.8 the number of
272 measurements for single samples ranges between 1 and 8 (with a median of 3), because this method can only assess the matric
273 head values after each reading of the respective sample states.

274 Hydraulic conductivity data obtained by the evaporation method range mostly from pF 1.0 to pF 3.2. Again, one single
275 conductivity data point originates from the air-entry of the porous cup for about half of the datasets. A separately measured
276 K_{sat} is available for 409 datasets. The data collection neither contains conductivity data in the range close to saturation (pF <1),
277 nor in the dry range. Currently, there is no standard laboratory method to determine hydraulic conductivity in this range. In the
278 online version in Figure 3 the different methods contributing to the retention and conductivity data are plotted as circles
279 (evaporation), triangles (air entry point), squares (dewpoint) and diamonds (K_{sat}). Figure 4 presents the same data colour coded
280 by bulk density.

281
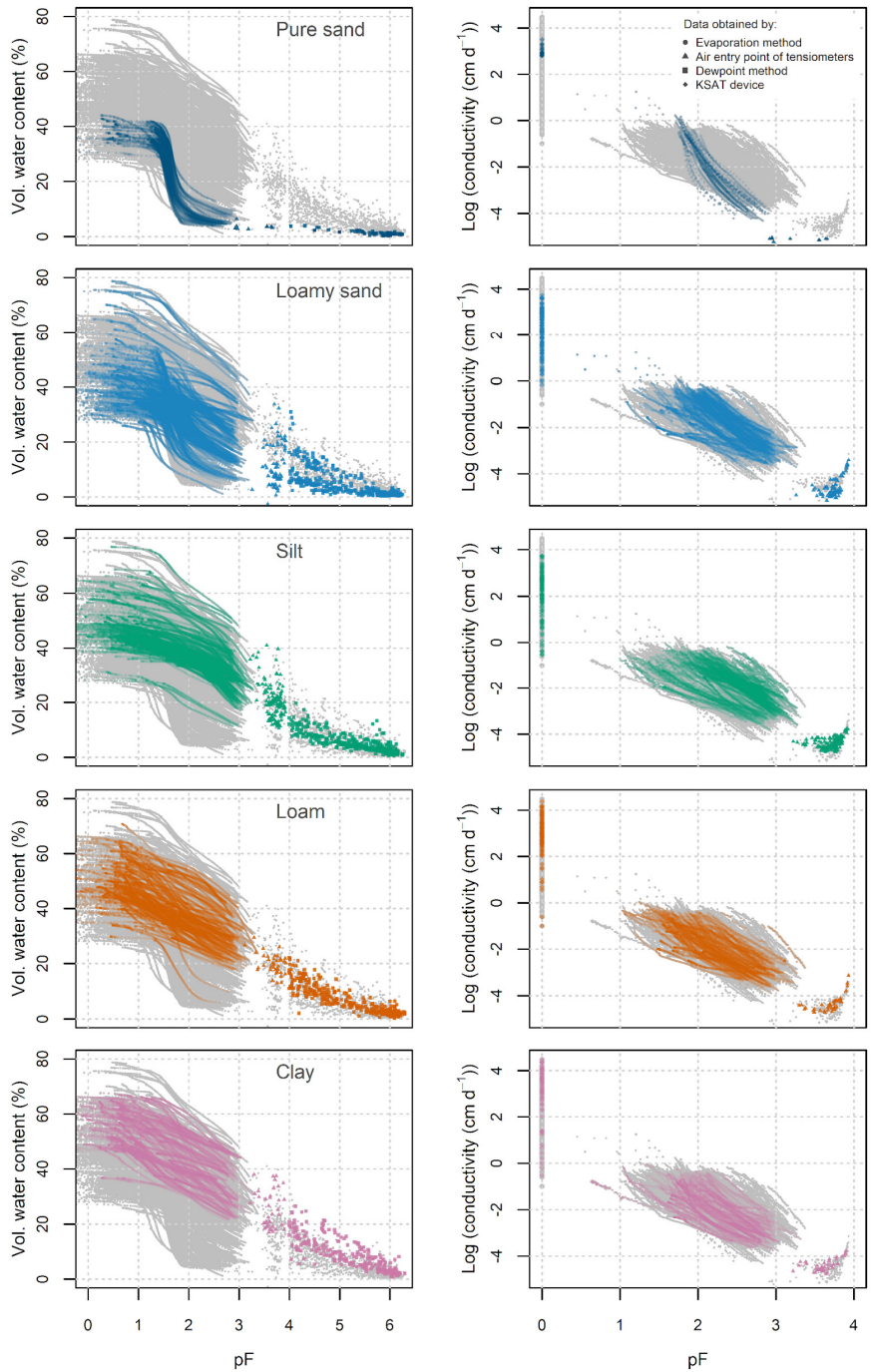
Figure 3: Soil water retention (left) and hydraulic conductivity (right) grouped and colour coded by texture class. Grey background symbols show all measured values. Please note the different pF ranges for the retention and conductivity curves. In the online version the different laboratory methods contributing to the retention and conductivity data are plotted as circles (evaporation), triangles (air entry point), squares (dewpoint) and diamonds (K_{sat}) visible after zooming in.
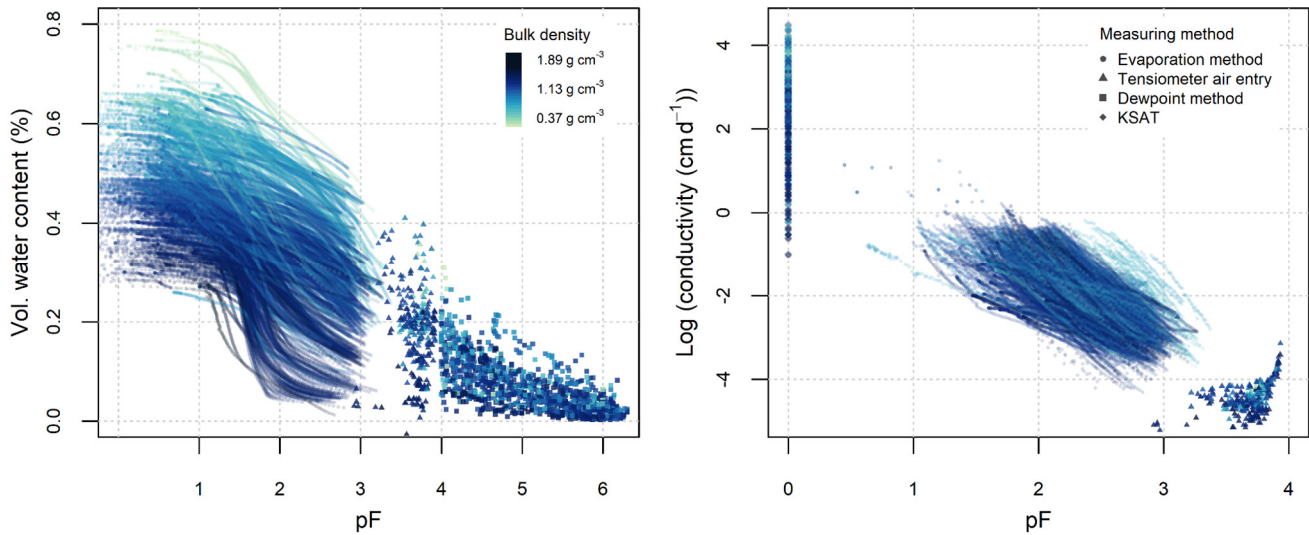
286
287 Figure 4: Soil water retention (left) and hydraulic conductivity (right) colour coded by bulk density. Please note the different pF
288 ranges for the retention and conductivity curves. A more detailed version with the used texture classes is in the Appendix Figure A2.
289 In the online version the different laboratory methods contributing to the retention and conductivity data are plotted as circles
290 (evaporation), triangles (air entry point), squares (dewpoint) and diamonds (K_{sat}) visible after zooming in.

291

3.4 Fitted SHP models

293 The distributions of the fitted model parameters for both VGM and PDI (data provided in table "Param.csv" in Hohenbrink et
294 al. (2023), but not shown here) mostly cover the predefined range of plausible parameters (Table 1). The constraining
295 boundaries were only hit in 5 cases except for parameter λ of the PDI model (154 cases in which bounds were hit).

296 The fitted water retention curves (Figure 5a and 5c) reflect the main characteristics of the measured SHP described above.
297 Retention curves from both models are similar in the wet to medium range. However, in the medium to dry moisture range
298 they systematically differ. The retention curves described by VGM approach a water content between 0% and 28%, while
299 those from the PDI model consistently reach zero saturation at $pF = 6.8$, which reflects the matric potential at oven dryness
300 (Schneider and Goss, 2012). The hydraulic conductivity curves described by VGM (Figure 5b) vary over a wide range. It
301 proves difficult to visually relate the curves to respective texture classes, because the wet range part scales strongly with the
302 existence of larger pores, and the shape of the curve is strongly limited by the underlying linear fit in log-log space. The PDI
303 model curves (Figure 5d) are more closely related to texture and span a much narrower range for each texture class. The
304 variation among the curves decreases towards the dry end of the saturation range. Especially in the dry range, the hydraulic
305 conductivity increases along the texture gradient from pure sand via loamy sand, silt and loam to clay. This phenomenon
306 results from the PDI model structure, where hydraulic conductivity in the dry range is directly derived from the water content
307 at $pF = 5.0$ (Peters et al., 2021). At $pF > 5.5$ the hydraulic conductivity of the PDI model is dominated by the isothermal
308 vapour conductivity for all texture classes.

As an estimate for soil water characteristics, we derived soil water content at field capacity (θ at $pF = 1.8$), soil water content at the permanent wilting point (θ at $pF = 4.2$), as well as the resulting plant available water content ($\theta(pF\ 1.8) - \theta(pF\ 4.2)$). Figure 6 shows these values in the texture triangle calculated based on the PDI retention curves. The water content at both, field capacity (Figure 6a) and wilting point (Figure 6b), roughly increases from sandy soils towards soils with finer textures. However, apart from this very general distinction, the values of both variables vary widely over the texture triangle, which directly results from the variation of the retention curves within a single texture class (Figure 5c). Plant available water content (Figure 6c) depicts the same high variability within the texture triangle. It varies between the extremes of 3.8 vol. % in pure sand up to 49.2 vol. % in fine-textured soil but does not align to any clear, texture-related pattern.
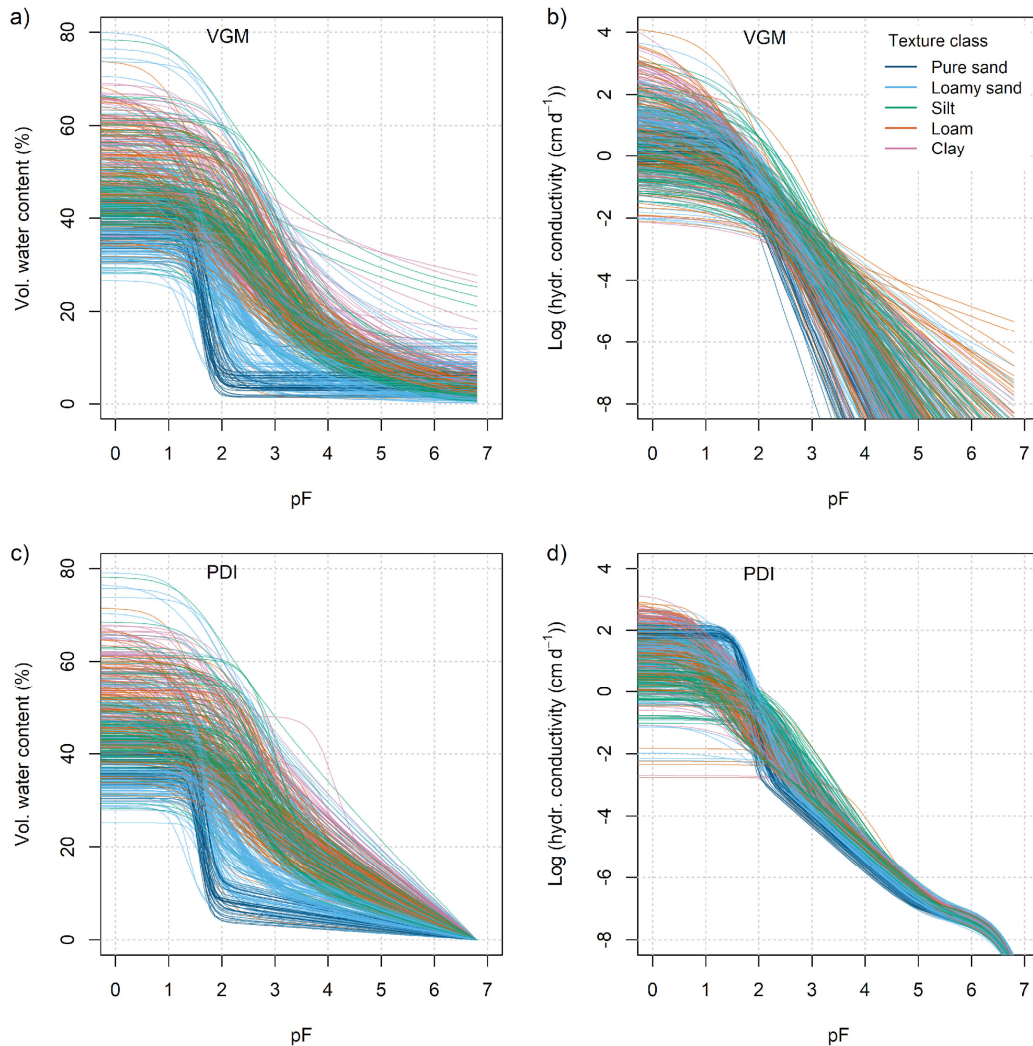
Figure 5: Retention curves (left, a and c) and hydraulic conductivity curves (right, b and d) for the van Genuchten-Mualem model (a and b) and the PDI model with VGM basic function (c and d). Soil texture classes are colour coded.

321
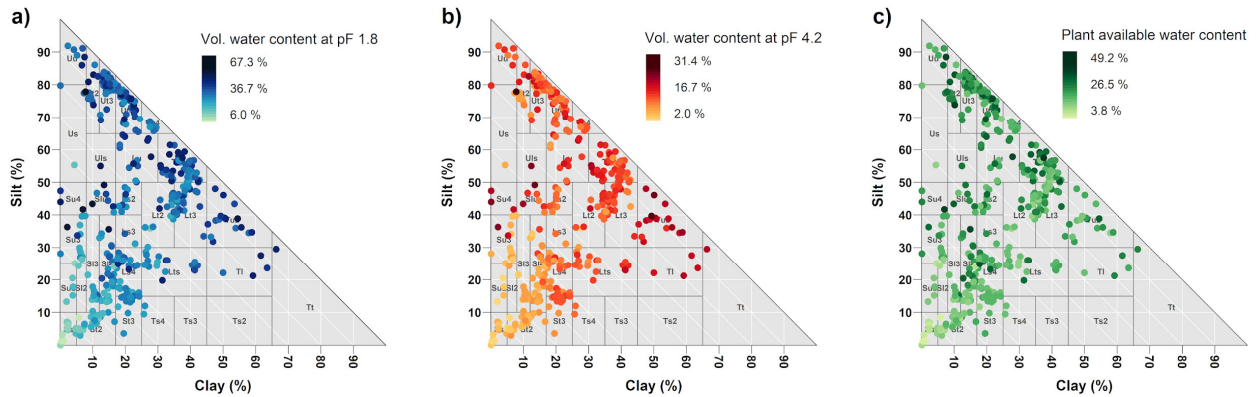
Figure 6: Volumetric water contents at (a) field capacity, (b) the plant wilting point, and (c) the resulting plant available water scattered on the soil texture triangle. The values provided in the data collection are calculated from retention curves described by the PDI model.

4 Discussion

4.1 New applications arising from the data collection

The combination of different state-of-the-art methods to measure soil water retention and hydraulic conductivity based on undisturbed samples yields a unique SHP data collection. Especially, the denser coverage of a wider range of saturation levels compared to existing data collections makes it valuable for new applications. For example, the retention data in the dry range measured with the dewpoint method represent essential information to develop retention models that overcome the concept of a residual water content, which has been shown to be not physically consistent (e.g. Schneider and Goss, 2012; Tuller and Or, 2005; Nimmo, 1991). Furthermore, this data collection provides measurements of both saturated and unsaturated hydraulic conductivity in high resolution and over a wide range of saturation levels. This supports the development and improvement of hydraulic conductivity models.

The high level of standardisation using the described methods enables us to link data from various labs without methodological offsets commonly found due to slightly deviating soil sample processing. Although the data set does not reach any global coverage, the data set exceeds existing SHP data collections by data density, extent of the values and variables, and consistency. We envision the proposed data structure as a foundation for upcoming additions with the methods becoming more and more accessible.

The VGM and PDI parameters provided in the data collection have been estimated with state-of-the-art techniques. Both parameter sets can be valuable to develop and test simulation models and to perform simulation studies. They can also serve as a benchmark for further developments of non-linear parameter estimation algorithms. We have intentionally omitted the measured K_{sat} values during parameter estimation. Considering K_{sat} in combination with unimodal SHP models usually causes

an overestimation of hydraulic conductivity close to saturation since the K_{sat} information mainly reflects the impact of soil structure (Durner, 1994; Peters et al., 2023). The K_s parameter derived for the PDI can thus be interpreted as the conductivity of the soil matrix only, excluding effects of soil structure, similarly to Weynants et al. (2009), and as further discussed in Fatichi et al. (2020). It is now possible to further investigate the relation between K_s of the soil matrix and K_{sat} of the entire soil including structure effects based on the parameters provided.

In addition to the commonly used three fractions sand, silt and clay to classify soil texture, we provide subgroups for sand and silt. Most pedotransfer functions only consider the three main texture groups as predictor variables. Our data suggests that the main texture classes alone contain limited information about soil hydrologic properties (large spread of hydraulic curves within texture classes in Figure 3, scattered texture distribution for plant available water in Figure 6c). Only in combination with bulk density and C_{org}, the data becomes more informative (Figure 4 and A2). For advancing pedotransfer functions, the presented data collection is a promising basis for analyses of (i) the resolution of texture data and texture class delineation (c.f. Twarakavi et al., 2010), (ii) the resolution of the SHP data series and (iii) suitable indicators for hydrologic functioning (field capacity, wilting point, etc. c.f. Assouline and Or, 2014).

4.2 Limitations of the data collection and further research needs

Although the data collection enables many different applications, it has some limitations that must be considered when analysing the data and interpreting the results. The single data sets are not completely statistically independent from each other for the following main reasons: (i) many samples stem from identical sites; (ii) some data sets exhibit identical texture and C_{org} values, because in these cases only few aggregated disturbed samples representative for a whole site have been taken; (iii) the analyses have been performed in five different laboratories. However, by closely following the guidelines of the experiments a high degree of standardisation in the laboratory protocols could be achieved.

In some situations, it might be reasonable to thin out the data by keeping only data sets assumed to be statistically independent. However, whether this is necessary depends on the particular research question and the applied data analysing technique. We have decided to include all available data sets and to provide enough meta information to evaluate the statistical dependencies and leave it up to the user to decide how to handle such dependencies.

Another limitation of the data that users must cope with is the unbalanced distribution of the datasets in terms of basic soil properties. For example, Luvisols with silt contents between 70 % and 85 % are overrepresented in the data collection due to their agricultural importance which led to more frequent soil analyses. In contrast, there are data gaps for the sandy clay and sandy silt texture classes, because they do occur more sparsely in the regions under study and are generally less intensively investigated. The unbalanced distribution of the data can be especially challenging for the development of pedotransfer functions. This problem can be best solved by supplementing the data collection by additional measurements, but this is a major task at the level of the soil hydrological community and can hardly be achieved by individual researchers.

At the level of individual datasets, the gaps in the hydraulic conductivity series near saturation and under dry conditions are another important limitation. Such data are needed to parameterize existing models in a way that they become more reliable

377 in the respective saturation ranges. More comprehensive hydraulic conductivity data is also required to develop new SHP
378 models. Therefore, we identify a need for developing and establishing new standard methods to measure hydraulic conductivity
379 close to saturation (Sarkar et al., 2019b, a) and in the dry range.

4.3 Implications for lab procedures and further extension of the data collection

381 The different texture class definitions required us to estimate the missing breakpoint between USDA sand and silt fractions
382 based on monotone cubic splines fitted to the German cumulative particle size distributions as recommended by Nemes et al.
383 (1999). While this technique appears perfectly feasible given the high level of detail in the texture data with seven classes, this
384 would have been more uncertain when the data would have been limited to the three main texture classes. The estimate can be
385 eliminated altogether, when the 63 µm sieve and the 50 µm sieve are included as standard.

386 Despite the high level of standardisation using the described techniques to determine SHPs, the quality check based on the
387 procedure presented in section 2.4 proved to be important to avoid erroneous interpretations and to ensure data quality. When
388 followed, data from different labs can be easily combined. It would be favourable if this could be extended to further relevant
389 soil properties e.g. soil texture, C_{org}, Mid-Infrared reflection spectra. We encourage the community to use and extend this data
390 collection.

5 Data availability

392 The data collection is hosted in the repository GFZ Data Services (Hohenbrink et al, 2023). It can be accessed via
393 https://doi.org/10.5880/fidgeo.2023.012. The final DOI will be registered when the paper is accepted, temporary data access
394 to Hohenbrink et al. (2023) via https://dataservices.gfz-
395 potsdam.de/panmetaworks/review/5c617cd2664ea4d03e81301b5bc2236f1948a3cf7eb9bad48da940524f0cbac0/. The rights
396 of use are defined by a creative common licence (CC BY 4.0). The data collection in the repository includes all data presented
397 in this paper. Further information and materials such as small volumes of air-dried reserve soil samples can be provided by the
398 corresponding author or the second author (Conrad.Jackisch@tbt.tu-freiberg.de) upon request.

6 Summary and conclusions

400 Motivated by a need for detailed soil water retention and hydraulic conductivity data, we collected data from 572 undisturbed
401 ring samples in a community initiative. High level of standardisation in new measurement techniques and rigorous quality
402 filtering allowed for consistency, which is rarely achieved in soil hydraulic analyses from different labs.

403 Initial comparisons of hydraulic indicators (e.g. plant available water content) with classical texture data showed very weak
404 predictive power by texture. The addition of more texture classes from the particle size distribution and the addition of
405 supplementary data on bulk density and organic carbon content appear to be more informative predictors.

The data collection can be used in its current form or integrated into existing data collections. All data sets were acquired directly from the original sources, which makes the data collection completely independent of the existing pool of data on SHP and thus contributes to their diversification. In particular, the hydraulic conductivity series will substantially expand the existing inventory of SHP data.

We expect that this data collection can serve as an independent, new and therefore unexplored benchmark reference to evaluate already existing SHP models and pedotransfer functions. Due to the high resolution of measured data compared to most data in existing databases and the extended range of saturation, it is also an ideal basis to develop and test new advanced SHP models and pedotransfer functions. It is well suited to verify findings and conclusions that have so far emerged from the existing data collections.

Author contributions

TH compiled and analysed the data, created the figures, and drafted the manuscript in close collaboration with CJ. All co-authors contributed to the final version. JM, JK, FL, and CJ provided already existing data sets and evaluated them initially. KG and MN collected samples with new combinations of basic soil properties, performed laboratory measurements, and evaluated them initially. AP adapted the PDI model and the fitting software, was involved in building the data collection, and supervised the project. WD and SI supported the data preparation and analyses.

Competing Interests

Conrad Jackisch is a member of the editorial board of Earth System Science Data. The authors have no other competing interests to declare.

Acknowledgements

The initiative of this data collection has emerged from a project funded by the Deutsche Forschungsgemeinschaft (DFG, German Research Foundation grant PE 1912/4-1). TH and MN were funded by the same project. JM was funded by the Collaborative Research Centre "AquaDiva", funded as DFG SFB 1076, project number 218627073. CJ and TH were part of the DFG research unit "From Catchments as Organised Systems to Models Based on Functional Units" (FOR 1598) funded as DFG grant ZE 533/9-1. We thank Birgit Walter and Ines Andrae for laboratory analyses of the soil samples taken especially for this initiative. All authors thankfully acknowledge their respective field and lab support. Without their meticulous work this data set would not have come into existence.

References

Ad-hoc-Arbeitsgruppe Boden: Bodenkundliche Kartieranleitung: mit 41 Abbildungen, 103 Tabellen und 31 Listen, edited by: Eckelmann, W., In Kommission: E. Schweizerbart'sche Verlagsbuchhandlung (Nägele und Obermiller), Stuttgart, 2005.

436 Assouline, S. and Or, D.: Conceptual and Parametric Representation of Soil Hydraulic Properties: A Review, VADOSE ZONE
437 J, 12, httSps://doi.org/10.2136/vzj2013.07.0121, 2013.

438 Assouline, S. and Or, D.: The concept of field capacity revisited: Defining intrinsic static and dynamic criteria for soil internal
439 drainage dynamics, Water Resources Research, 50, 4787–4802, https://doi.org/10.1002/2014wr015475, 2014.

440 Brooks, R. H. and Corey, A. T.: Hydraulic properties of porous media, Colorado State University, Fort Collins, Colorado,
441 1964.

442 Campbell, G. S., Smith, D. M., and Teare, B. L.: Application of a Dew Point Method to Obtain the Soil Water Characteristic,
443 in: Experimental unsaturated soil mechanics, Springer, 71–77, https://doi.org/10.1007/3-540-69873-6_7, 2007.

444 Carsel, R. F. and Parrish, R. S.: Developing joint probability distributions of soil water retention characteristics, WATER
445 RESOUR RES, 24, 755–769, https://doi.org/10.1029/WR024i005p00755, 1988.

446 Duan, Q., Sorooshian, S., and Gupta, V.: Effective and efficient global optimization for conceptual rainfall-runoff models.
447 WATER RESOUR RES. 28, 1015–1031, https://doi.org/10.1029/91WR02985, 1992.

448 Durner, W.: Hydraulic conductivity estimation for soils with heterogeneous pore structure, WATER RESOUR RES, 30, 211–
449 223, https://doi.org/10.1029/93WR02676, 1994.

450 Durner, W., Iden, S.C.: The improved integral suspension pressure method (ISP+) for precise particle size analysis of soil and
451 sedimentary materials, SOIL TILL RES, 213, 105086, https://doi.org/10.1016/j.still.2021.105086, 2021.

452 Durner, W., Iden, S.C., von Unold, G.: The integral suspension pressure method (ISP) for precise particle-size analysis by
453 gravitational sedimentation, WATER RESOUR RES, 53, 33–48, https://doi.org/10.1002/2016WR019830, 2017.

454 Fatichi, S., Or, D., Walko, R., Vereecken, H., Young, M. H., Ghezzehei, T. A., Hengl, T., Kollet, S., Agam, N., and Avissar,
455 R.: Soil structure is an important omission in Earth System Models, NAT COMMUN, 11, 1–11,
456 https://doi.org/10.1038/s41467-020-14411-z, 2020.

457 Van Genuchten, M. T.: A Closed-form Equation for Predicting the Hydraulic Conductivity of Unsaturated Soils, SOIL SCI
458 SOC AM J, 44, 892–898, https://doi.org/10.2136/sssaj1980.03615995004400050002x, 1980.

459 Germer, K. and Braun, J.: Multi-step outflow and evaporation experiments–Gaining large undisturbed samples and comparison
460 of the two methods, J HYDROL, 577, 123914, https://doi.org/10.1016/j.jhydrol.2019.123914, 2019.

461 Gupta, S., Papritz, A., Lehmann, P., Hengl, T., Bonetti, S., and Or, D.: Global Soil Hydraulic Properties dataset based on
462 legacy site observations and robust parameterization, Scientific Data, 9, 1–15, https://doi.org/10.1038/s41597-022-01481-5,
463 2022.

464 Iden, S. C., Peters, A., and Durner, W.: Improving prediction of hydraulic conductivity by constraining capillary bundle models
465 to a maximum pore size, ADV WATER RESOUR, 85, 86–92, https://doi.org/10.1016/j.advwatres.2015.09.005, 2015.

466 Hohenbrink, T. L., Jackisch, C., Durner, W., Germer, K., Iden, S. C., Kreiselmeier, J., Leuther, F., Metzger, J. C., Naseri, M.,
467 Peters, A.: Soil hydraulic characteristics in a wide range of saturation and soil properties. GFZ Data Services.
468 https://doi.org/10.5880/fidgeo.2023.012, 2023. DOI registration when the paper is accepted, temporary data access via
469 https://dataservices.gfz-
470 potsdam.de/panmetaworks/review/5c617cd2664ea4d03e81301b5bc2236f0c9620ca0bed66c726d2e424d166fd85/.

Jackisch, C., Angermann, L., Allroggen, N., Sprenger, M., Blume, T., Tronicke, J., and Zehe, E.: Form and function in hillslope hydrology: in situ imaging and characterization of flow-relevant structures, HYDROL EARTH SYST SC, https://doi.org/10.5194/hess-21-3749-2017, 2017.

Jackisch, C., Germer, K., Graeff, T., Andrä, I., Schulz, K., Schiedung, M., Haller-Jans, J., Schneider, J., Jaquemotte, J., Helmer, P., and others: Soil moisture and matric potential–an open field comparison of sensor systems, EARTH SYST SCI DATA, 12, 683–697, https://doi.org/10.5194/essd-12-683-2020, 2020.

Jarvis, N. J.: A review of non-equilibrium water flow and solute transport in soil macropores: principles, controlling factors and consequences for water quality, SOIL SCI., 58, 523-546, https://doi.org/10.1111/j.1365-2389.2007.00915.x, 2007.

Kirste, B., Iden, S. C., and Durner, W.: Determination of the Soil Water Retention Curve around the Wilting Point: Optimized Protocol for the Dewpoint Method, SOIL SCI SOC AM J, 83, 288–299, https://doi.org/10.2136/sssaj2018.08.0286, 2019.

Köhn, M.: Die mechanische Analyse des Bodens mittels Pipettmethode. Z PFLANZ BODENKUNDE, 21 (2), 211–222, https://doi.org/10.1002/jpln.19310210206, 1931.

Kreiselmeier, J., Chandrasekhar, P., Weninger, T., Schwen, A., Julich, S., Feger, K.-H., and Schwärzel, K.: Quantification of soil pore dynamics during a winter wheat cropping cycle under different tillage regimes, SOIL TILL RES, 192, 222–232, https://doi.org/10.1016/j.still.2019.05.014, 2019.

Kreiselmeier, J., Chandrasekhar, P., Weninger, T., Schwen, A., Julich, S., Feger, K.-H., and Schwärzel, K.: Temporal variations of the hydraulic conductivity characteristic under conventional and conservation tillage, GEODERMA, 362, 114127, https://doi.org/10.1016/j.geoderma.2019.114127, 2020.

Leuther, F., Schlüter, S., Wallach, R., and Vogel, H.-J.: Structure and hydraulic properties in soils under long-term irrigation with treated wastewater, GEODERMA, 333, 90–98, https://doi.org/10.1016/j.geoderma.2018.07.015, 2019.

Van Looy, K., Bouma, J., Herbst, M., Koestel, J., Minasny, B., Mishra, U., Montzka, C., Nemes, A., Pachepsky, Y. A., Padarian, J., and others: Pedotransfer Functions in Earth System Science: Challenges and Perspectives, REV GEOPHYS, 55, 1199–1256, https://doi.org/10.1002/2017RG000581, 2017.

Metzger, J. C., Filipzik, J., Michalzik, B., and Hildebrandt, A.: Stemflow Infiltration Hotspots Create Soil Microsites Near Tree Stems in an Unmanaged Mixed Beech Forest, FRONT FOR GLOB CHANGE, 4, 701293, https://doi.org/10.3389/ffgc.2021.701293, 2021.

Moeys, J.: soiltexture: Functions for Soil Texture Plot, Classification and Transformation. R package version 1.5.1. https://CRAN.R-project.org/package=soiltexture, 2018.

Moshrefi, N.: A new method of sampling soil suspension for particle-size analysis, SOIL SCI., 155, 245–248, https://doi.org/10.1097/00010694-199304000-00002, 1993.

Mualem, Y.: A New Model for Predicting the Hydraulic Conductivity of Unsaturated Porous Media, WATER RESOUR RES, 12, 513–522, https://doi.org/10.1029/WR012i003p00513, 1976.

Nemes, A., Schaap, M., Leij, F., and Wösten, J.: Description of the unsaturated soil hydraulic database UNSODA version 2.0, J HYDROL, 251, 151–162, https://doi.org/10.1016/S0022-1694(01)00465-6, 2001.

505 Nemes, A., Wösten, J. H. M., Lilly, A., Oude Voshaar, J.H.: Evaluation of different procedures to interpolate particle-size
506 distributions to achieve compatibility within soil databases. GEODERMA, 90, 187-202. https://doi.org/10.1016/S0016-
507 7061(99)00014-2, 1999.

508 Nimmo, J. R.: Comment on the treatment of residual water content in "A consistent set of parametric models for the two-phase
509 flow of immiscible fluids in the subsurface" by L. Luckner et al., WATER RESOUR RES, 27, 661–662,
510 https://doi.org/10.1029/91WR00165, 1991.

511 Ottoni, M. V., Ottoni Filho, T. B., Schaap, M. G., Lopes-Assad, M. L. R., and Rotunno Filho, O. C.: Hydrophysical Database
512 for Brazilian Soils (HYBRAS) and Pedotransfer Functions for Water Retention, VADOSE ZONE J, 17,
513 https://doi.org/10.2136/vzj2017.05.0095, 2018.

514 Pertassek, T., Peters, A., and Durner, W.: HYPROP-FIT software user's manual, V. 3.0, UMS GmbH, Munich, Germany,
515 2015.

516 Peters, A.: Simple consistent models for water retention and hydraulic conductivity in the complete moisture range, WATER
517 RESOUR RES, 49, 6765–6780, https://doi.org/10.1002/wrcr.20548, 2013.

518 Peters, A. and Durner, W.: Simplified evaporation method for determining soil hydraulic properties, J HYDROL, 356, 147–
519 162, https://doi.org/10.1016/j.jhydrol.2008.04.016, 2008.

520 Peters, A. and Durner, W.: SHYPFIT 2.0 User's Manual. Research Report. Institut für Ökologie, Technische Universität
521 Berlin, Germany., 2015.

522 Peters, A., Hohenbrink, T. L., Iden, S. C., and Durner, W.: A Simple Model to Predict Hydraulic Conductivity in Medium to
523 Dry Soil From the Water Retention Curve, WATER RESOUR RES, e2020WR029211,
524 https://doi.org/10.1029/2020WR029211, 2021.

525 Peters, A., Hohenbrink, T. L., Iden, S. C., Genuchten, M. T. van, and Durner, W.: Prediction of the absolute hydraulic
526 conductivity function from soil water retention data, HYDROL EARTH SYST SC, 27, 1565–1582,
527 https://doi.org/10.5194/hess-27-1565-2023, 2023.

528 R Core Team: R: A Language and Environment for Statistical Computing, R Foundation for Statistical Computing, Vienna,
529 Austria. URL https://www.R-project.org/, 2020.

530 Sarkar, S., Germer, K., Maity, R., and Durner, W.: Measuring near-saturated hydraulic conductivity of soils by quasi unit-
531 gradient percolation—1. Theory and numerical analysis, J PLANT NUTR SOIL SC, 182, 524–534,
532 https://doi.org/10.1002/jpln.201800382, 2019a.

533 Sarkar, S., Germer, K., Maity, R., and Durner, W.: Measuring near-saturated hydraulic conductivity of soils by quasi unit-
534 gradient percolation—2. Application of the methodology, J PLANT NUTR SOIL SC, 182, 535–540,
535 https://doi.org/10.1002/jpln.201800383, 2019b.

536 Schaap, M. G., Leij, F. J., and Van Genuchten, M. T.: ROSETTA: a computer program for estimating soil hydraulic parameters
537 with hierarchical pedotransfer functions, J HYDROL, 251, 163–176, https://doi.org/10.1016/S0022-1694(01)00466-8, 2001.

538 Schindler, U.: Ein Schnellverfahren zur Messung der Wasserleitfähigkeit im teilgesättigten Boden an Stechzylinderproben,
539 Arch. Acker- u. Pflanzenbau u. Bodenkd., Berlin, 24, 1–7, 1980.

Schindler, U., Durner, W., Von Unold, G., Mueller, L., and Wieland, R.: The evaporation method: Extending the measurement range of soil hydraulic properties using the air-entry pressure of the ceramic cup, J PLANT NUTR SOIL SC, 173, 563–572, https://doi.org/10.1002/jpln.200900201, 2010.

Schindler, U. G. and Müller, L.: Soil hydraulic functions of international soils measured with the Extended Evaporation Method (EEM) and the HYPROP device, Open Data Journal for Agricultural Research, 3, https://doi.org/10.18174/odjar.v3i1.15763, 2017.

Schneider, M. and Goss, K.-U.: Prediction of the water sorption isotherm in air dry soils, GEODERMA, 170, 64–69, https://doi.org/10.1016/j.geoderma.2011.10.008, 2012.

Tuller, M. and Or, D.: Water films and scaling of soil characteristic curves at low water contents, WATER RESOUR RES, 41, https://doi.org/10.1029/2005WR004142, 2005.

Twarakavi, N. K. C., Šimůnek, J., and Schaap, M. G.: Can texture-based classification optimally classify soils with respect to soil hydraulics?, Water Resour Res, 46, https://doi.org/10.1029/2009wr007939, 2010.

USDA: Soil Taxonomy: A Basic System of Soil Classification for Making and Interpreting Soil Surveys, 2nd edition, United States Department of Agriculture, Washington DC, USA, 1999.

Vereecken, H., Weynants, M., Javaux, M., Pachepsky, Y., Schaap, M., and Genuchten, M. T.: Using Pedotransfer Functions to Estimate the van Genuchten–Mualem Soil Hydraulic Properties: A Review, VADOSE ZONE J, 9, 795–820, https://doi.org/10.2136/vzj2010.0045, 2010.

Weihermüller, L., Lehmann, P., Herbst, M., Rahmati, M., Verhoef, A., Or, D., Jacques, D., and Vereecken, H.: Choice of Pedotransfer Functions Matters when Simulating Soil Water Balance Fluxes, J ADV MODEL EARTH SY, 13, e2020MS002404, https://doi.org/10.1029/2020MS002404, 2021.

Weynants, M., Vereecken, H., and Javaux, M.: Revisiting Vereecken Pedotransfer Functions: Introducing a Closed-Form Hydraulic Model, VADOSE ZONE J, 8, 86–95, https://doi.org/10.2136/vzj2008.0062, 2009.

Weynants, M., Montanarella, L., Toth, G., Arnoldussen, A., Anaya Romero, M., Bilas, G., Borresen, T., Cornelis, W., Daroussin, J., Gonçalves, M. D. C., and others: European HYdropedological Data Inventory (EU-HYDI), EUR Scientific and Technical Research Series, https://doi.org/10.2788/5936, 2013.

Wilkinson, M. D., Dumontier, M., Aalbersberg, I. J., Appleton, G., Axton, M., Baak, A., Blomberg, N., Boiten, J.-W., Silva Santos, L. B. da, Bourne, P. E., Bouwman, J., Brookes, A. J., Clark, T., Crosas, M., Dillo, I., Dumon, O., Edmunds, S., Evelo, C. T., Finkers, R., Gonzalez-Beltran, A., Gray, A. J. G., Groth, P., Goble, C., Grethe, J. S., Heringa, J., Hoen, P. A. C. t, Hooft, R., Kuhn, T., Kok, R., Kok, J., Lusher, S. J., Martone, M. E., Mons, A., Packer, A. L., Persson, B., Rocca-Serra, P., Roos, M., Schaik, R. van, Sansone, S.-A., Schultes, E., Sengstag, T., Slater, T., Strawn, G., Swertz, M. A., Thompson, M., Van Der Lei, J., Van Mulligen, E., Velterop, J., Waagmeester, A., Wittenburg, P., Wolstencroft, K., Zhao, J., and Mons, B.: Comment: The FAIR Guiding Principles for scientific data management and stewardship, Scientific Data, 3, https://doi.org/10.1038/sdata.2016.18, 2016.

Wösten, J., Lilly, A., Nemes, A., and Le Bas, C.: Development and use of a database of hydraulic properties of European soils, GEODERMA, 90, 169–185, https://doi.org/10.1016/S0016-7061(98)00132-3, 1999.

Zhang, Y. and Schaap, M. G.: Weighted recalibration of the Rosetta pedotransfer model with improved estimates of hydraulic parameter distributions and summary statistics (Rosetta3), J HYDROL, 547, 39–53, https://doi.org/10.1016/j.jhydrol.2017.01.004, 2017.

578 Zhang, Y., Weihermüller, L., Toth, B., Noman, M., and Vereecken, H.: Analyzing dual porosity in soil hydraulic properties
579 using soil databases for pedotransfer function development, VADOSE ZONE J, e20227, https://doi.org/10.1002/vzj2.20227,
580 2022.

581

Appendix

583 Since global coverage and regional distribution of the sampling has not been a criterion for data collection, the samples are

584 basically linked to the research activities of the contributors. Most samples have been taken in Central Europe (n = 508). A

585 few data sets come from Canada (n = 29), Japan (n = 5) and Israel (n = 30) (Figure A1 for visual reference).

586

587
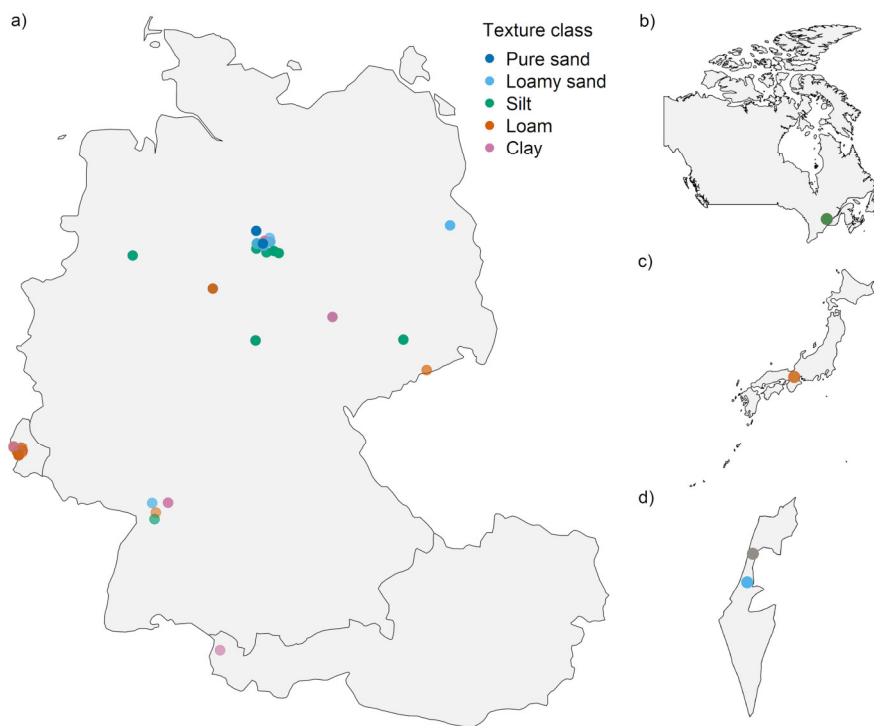
Figure A1: Locations of the sampling sites in (a) Luxembourg, Germany and Austria, (b) Canada, (c) Japan, and (d) Israel. Please note that the map scales differ, as the maps should only provide a broad overview.

590

591 Because soil texture classes did not provide strong information about the soil water retention and hydraulic conductivity curves,

592 we have added the same plots as in Figure 3 colour-coded by bulk density (Figure A2).

593
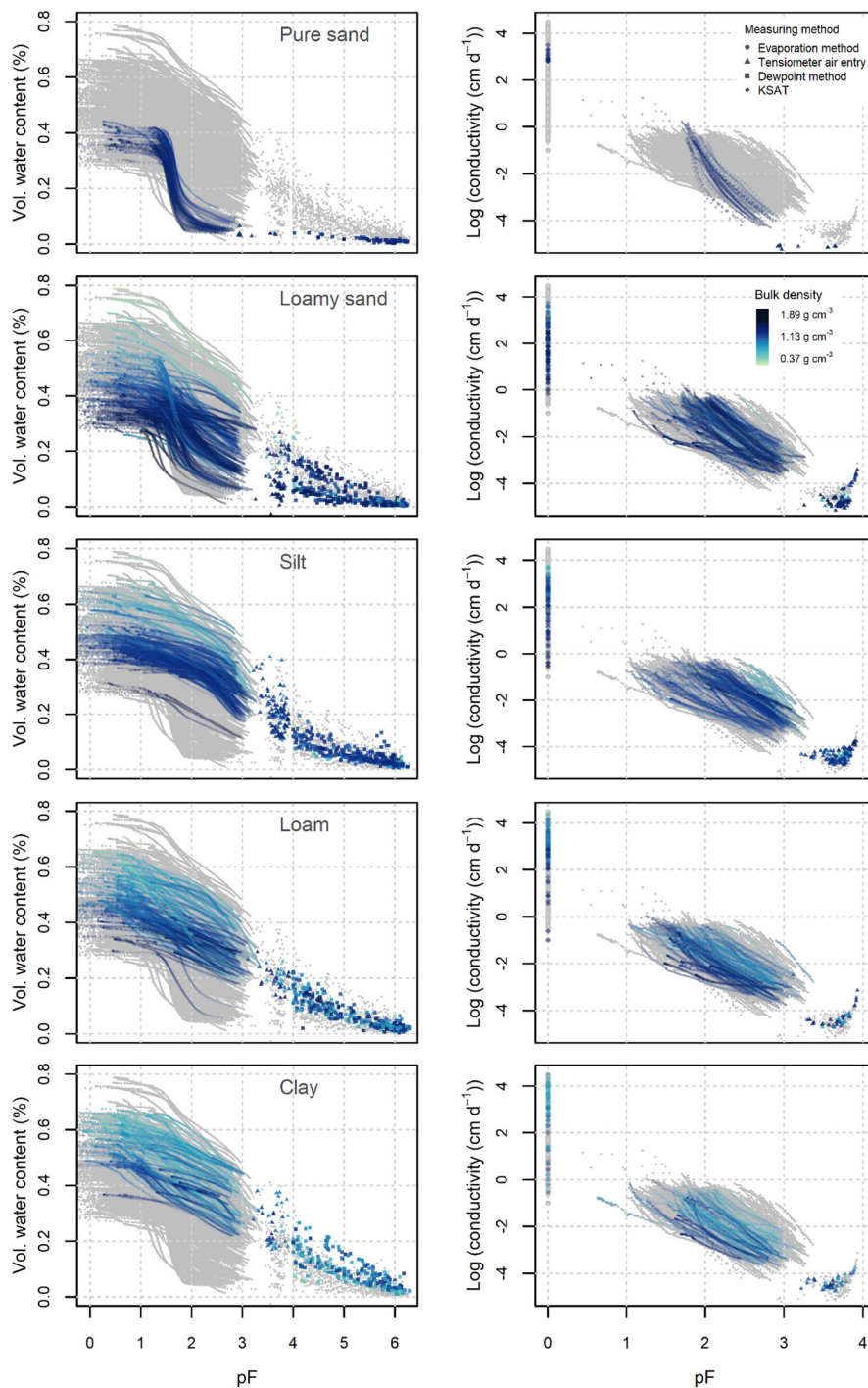
Figure A2: Soil water retention (left) and hydraulic conductivity (right) colour coded by bulk density. Please note the different pF ranges for the retention and conductivity curves. In the online version the different methods contributing to the retention and conductivity data are plotted as circles (evaporation), triangles (air entry point), squares (dewpoint) and diamonds (K_{sat}).